IOSR Journal Of Applied Physics (IOSR-JAP)
e-ISSN: 2278-4861.Volume 15, Issue 2 Ser. III (Mar. – Apr. 2023), PP 01-09
www.Iosrjournals.Org

Electrical Investigation of Pure and Silver, Zinc and PVP doped Tin Oxide Nanocomposites

R. Sudha Periathai[1]*, A. Amutha[1]*, T. Mohana Priya[1], S. Rufin Evangalin[1]
[1](*Department of Physics, The Standard Fireworks Rajaratnam College for Women (Autonomous), Sivakasi, India)*

Abstract:
Pure and Zn, PVP and Ag doped tin oxide nanoparticles were prepared by microwave assisted chemical co-precipitation method. The influence of zinc, PVP and Ag nanoparticles in tin oxide is obtained by X-ray Diffraction pattern and Electrical conductivity studies. The Ag and Zn ions replaced the tin ions in tin oxide lattice sites. Therefore, no zinc and silver peaks are observed in XRD. There is no impurity peak observed in XRD. The X-ray diffraction pattern reveals the tetragonal rutile structure of tin oxide nanoparticles. Increasing the doping concentration of zinc in tin oxide decrease the crystalline size. The band gap of pure and zinc, PVP and Ag doped tin oxide nanoparticles are calculated from Diffuse reflectance spectroscopy.The conductivity studies of the doped samples is increased due to the Ag nanoparticles.
Key Word*: UV-Visible absorption spectroscopy, SnO2 nanoparticles, Conductivity, Bandgap.*

Date of Submission: 14-04-2023 Date of Acceptance: 27-04-2023

I. Introduction

Inorganic particles with polymers are used to produce novel materials which are tuned their properties. These are different from the constituent polymers. Hence, these materials are used in composites, adhesives, plastics and rubbers[1]. Therefore, the polymers are classified as miscible or immiscible blend polymers due to the level of molecular mixing[2]. Also, these nanocomposites exist due to the interactions of dipole – dipole forces, bonding of hydrogen atom and the charge transfer between the molecules. Now a days most of the materials are based on inorganic nanoparticles implanted blend polymer nanocomposites. Hence, this kind of addition of inorganic particles in nanocomposites plays the significant role to enhance their properties in wide range of applications.

Among all other polymers, the PVP and PVA are widely used in the synthesis of metal oxide nanoparticles. Poly (vinyl alcohol) (PVA) and PVP are having hydroxyl group and carbon chain which are producing interpenetrating network in the polymer nanocomposites[3]. Also, the Polyvinyl pyrrolidone (PVP) is used as a capping agent to regulate the growth of metals and metal oxide nanoparticles[4]. Particularly, PVP is widely used to the preparation of homogeneous structured nanoparticles. Also, the important applications of PVP are to prevent the aggregation of nanoparticles and to maintain the stabilization of nanoparticles[5].

Metal oxide nanoparticles are used in wide range of applications such as solar cells, light emitting diodes, gas sensors, etc., There are variety of metal oxides are available now a days. But, all the other metal oxides, tin oxide is the special semiconductor due to their transparent property. Metal doping enhances the properties of metal oxide materials. Zn and Sn ionic radius are similar. Therefore, the doping Zn in tin oxide does not produce the drastic changes but it is used to create the greater number of oxygen vacancy to enhance the electrical property and gas sensor applications.

Particularly, novel metal doped semiconductor oxide enormously tuned their properties. Hence, these materials are easily enhanced their optical and electrical properties[6]. Especially, doping of silver nanoparticles are playing significant role to enhance the optical property due to their surface plasmon resonance[7]. Also, silver nanoparticles are used to tune the morphology and size of the nanoparticles[8].

There are different methods are used to prepare the semiconductor oxide materials such as hydrothermal, sol-gel, solvothermal, microwave assisted co-precipitation and chemical co-precipitation methods[9,10,11]. The microwave assisted co-precipitation is the simplest and cheapest method to synthesis the nanoparticles. The present study Zn, PVP, and Ag doped tin oxide nanoparticles are prepared by microwave assisted co-precipitation method. The prepared nanoparticles are characterized by X-ray Diffraction, UV-Visible absorption spectroscopy and impedance spectroscopy.

II. Material And Methods

2.1 Synthesis of SnO2 nanoparticles

A 0.1M of $SnCl_2.2H_2O$ was taken and added to double distilled water and subjected to stirring. A 0.5g PVP was allowed to mix in 10ml of double distilled water and it was slowly added to the $SnCl_2.2H_2O$ solution. Required ammonia solution was slowly added to the $SnCl_2.2H_2O$solution. After vigorous stirring, the sample was kept in microwave oven to obtain the precipitate. The precipitate was centrifuged using water to remove the impurities. Finally, the prepared sample was dried using microwave oven. The similar procedure was followed for the synthesis of Zn doped SnO_2 nanoparticles.

2.1 Synthesis of Zn, Ag and PVP doped SnO2 nanoparticles

The doped samples were prepared by varying the zinc concentration keeping the same silver and PVP concentration. A 0.1M of $ZnCl_2$ and 0.9M of $SnCl_2.2H_2O$, 0.2M of $ZnCl_2$ and 0.8M of $SnCl_2.2H_2O$, 0.3M of $ZnCl_2$ and 0.7M of$SnCl_2.2H_2O$ was taken to prepare Doped1 (D1), Doped2 (D2) and Doped3 (D3) respectively. A 0.02g of silver was added to all doped samples. The required ammonia and 0.5g of PVP was also added one by one slowly into the mixed Zinc chloride and tin chloride solution. The same procedure was followed to prepare all the doped samples.

III. Result and Discussions

3.1 X-ray Diffraction study:

Figure 1 shows the XRD pattern of pure SnO2 and Ag, Zn & PVP doped SnO_2 nanoparticles
XRD study is a technique used to identify the crystalline phases, size, orientation and lattice parameter of the prepared samples. From Figure 1 it is observed that the XRD patterns reveal the tetragonal structure of tin oxide nanoparticles.

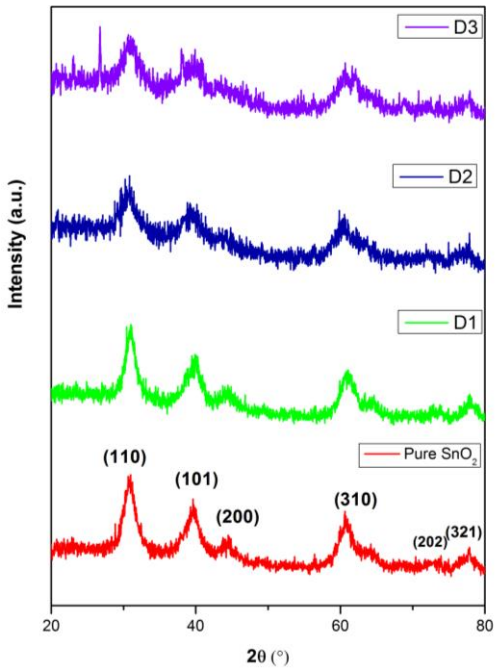

Fig. 1.XRD pattern of pure SnO2 and Ag, Zn & PVP doped SnO_2 nanoparticles

There are no separate impurity peaks observed in pure and doped samples. Therefore, the zinc and silver nanoparticles replaced tin atoms in tin oxide nanoparticles. Hence, a greater number of oxygen vacancies are created in doped samples when compared to pure tin oxide nanoparticles. There is no separate peak is observed for PVP. Because, PVP is always used as capping agent to tune the size, morphology and product agglomeration of nanoparticles.[12] In this case, PVP and tin oxide nanocomposites are formed in pure and doped nanoparticles.

UV- Visible absorption spectroscopy study

The absorption peak at 383 nm is ascribed due to the composition of PVP and pure tin oxide nanoparticles which is shown in fig. 2. The UV-Visible absorption spectra of Ag, Zinc and PVP doped tin oxide nanoparticle is shown in fig. 3. The peak broadening observed in the range from 364 nm to 484 nm for D1, D2, D3 and D4 samples due to the Surface Plasmon Resonance of Silver nanoparticles. Hence, the silver nanoparticles are presented in the prepared samples. The absorption intensity is decreased with the increasing concentration of doped materials. There is no separate PVP absorption peak is observed in Fig. 2 and Fig. 3. But the PVP plays the main role to reduce $AgNO_3$ to Ag nanoparticles. The strong absorption peak is observed at 383 nm for pure SnO_2 nanoparticles[13].

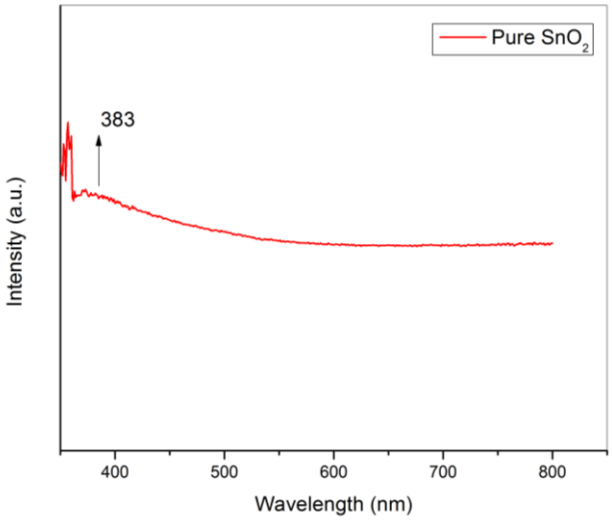

Fig. 2. UV- Absorption spectra for Pure Tin oxide nanoparticles

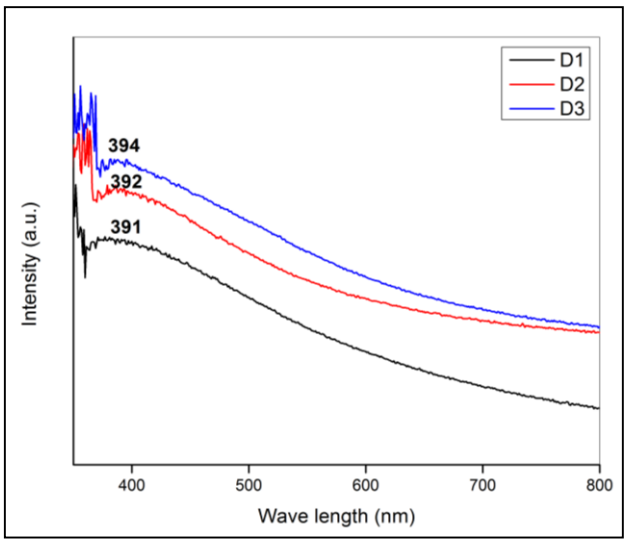

Fig. 3. UV- Absorption spectra of Zinc, PVP and Silver doped Tin Oxide nanoparticles

Diffuse reflectance spectroscopy:

The band gap is obtained from the Kubelka-Munk function. The band gap value of pure tin oxide is 2.94 eV is shown in Fig. 4. The band gap value of doped samples is 3.20, 3.28, 3.31 and 3.36 eV are tabulated in Table 1. Hence, the band gap is increased with increasing concentration of zinc ions in tin oxide when compared to pure tin oxide which is shown in Fig. 5. In diffuse reflectance spectroscopy, the Kubelka-Munk function were implemented to found the value of optical band gap of Pure SnO2 and Zn, PVP, Ag doped SnO2 nanoparticles. The Kubelka- Munk function is given by the following relation:

$$\mathbf{F(R)}=\frac{(1-R)^2}{2R} = \frac{K}{S}$$

Where,
F(R) is the Kubelka-Munk function which corresponds to absorbance,R is the reflectance,
K is the absorption coefficient, S is the scattering coefficient.

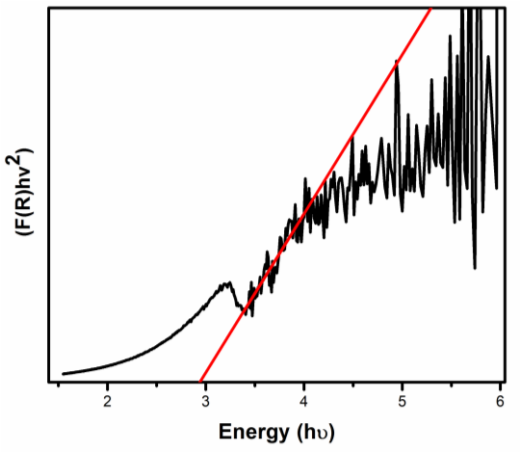

Fig. 4. Diffuse reflectance spectra represented in Kubelka–Munk function of Pure tin oxide nanoparticle

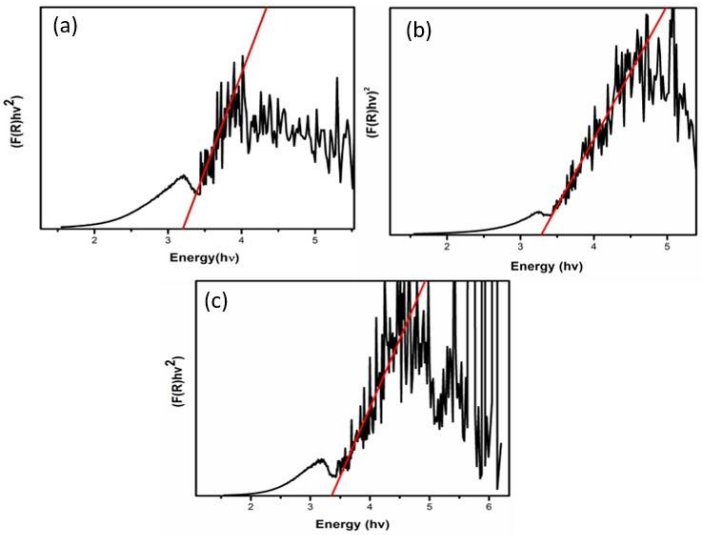

Fig. 5. Diffuse reflectance spectra represented in Kubelka–Munk function of doped tin oxide nanoparticles.

Table 1. The bandgap of pure nano particles and zinc, PVP, silver doped tin oxide nanoparticles

Prepared Samples	Bandgap(eV)
Pure SnO_2	2.94
Doped 1	3.20
Doped 2	3.28
Doped 3	3.31

Dielectric spectra for pure and zinc, PVP and silver doped tin oxide nanoparticles has been acquired. The dielectric constant (k) of samples is calculated, by the ratio of its permittivity (ε') to the permittivity of vacuum (ε"). The dielectric properties of every nanoparticles can be described by the real and imaginary parts of the compound permittivity (ε^*)
$\varepsilon^*=\varepsilon'(\omega)-i\varepsilon''(\omega)$
Here, $\varepsilon(\omega) \Longrightarrow$real factor (dielectric constant)
$\varepsilon''(\omega) \Longrightarrow$imaginary factor(dielectric loss)

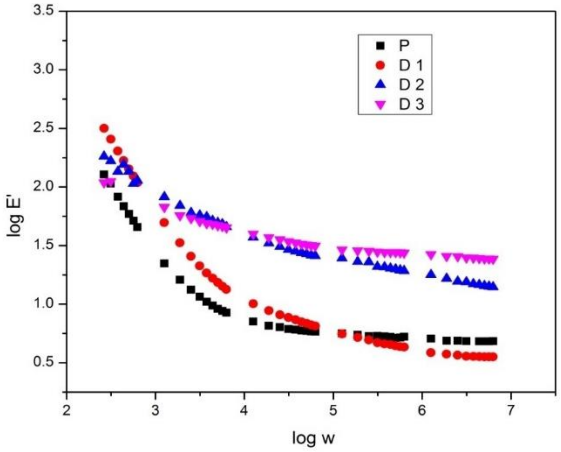

Fig. 6. The real part of dielectric permittivity and frequency for pure and doped tin oxide nanoparticles.

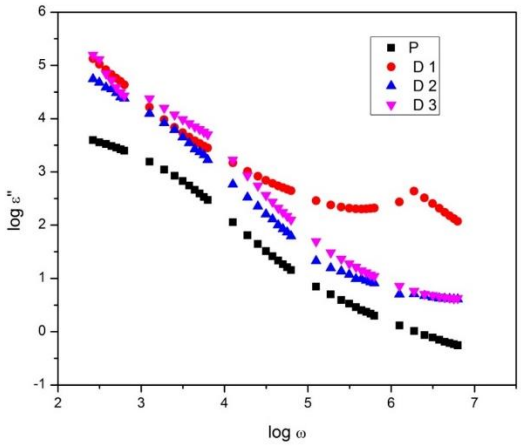

Fig. 7. The imaginary part of dielectric permittivity and frequency for pure and doped tin oxide nanoparticles.

Fig. 6. shows the deviation of the real a part of impedance (Z') as consequences of frequency. It is detected that Z decreases with increase in frequency for all compositions. It's due to increase in conductivity with frequency resultant from hopping phenomenon. The imaginary part of permittivity has been decreases with increase in zinc concentration at low frequency are shown in fig. 7. This is mainly due to the tiny material polarizability nature of zinc ions when replaces the tin ions. Therefore, increasing the dopant concentration of zinc ions may be the reason to decrease the material polarization. Hence, the material constant is decreased successively.

Conductance Spectra Analysis:

From the conductance spectra analysis, the dc conductivity has been determined for pure and doped tin oxide nanoparticles. The conductivity is increased with increasing the various concentrations of zinc ions. The Ag metal ions also the main reason for the drastic changing of conductivity. The Plasmon resonance is observed in UV-visible absorption spectroscopy which confirmed the presence of silver in the doped samples.

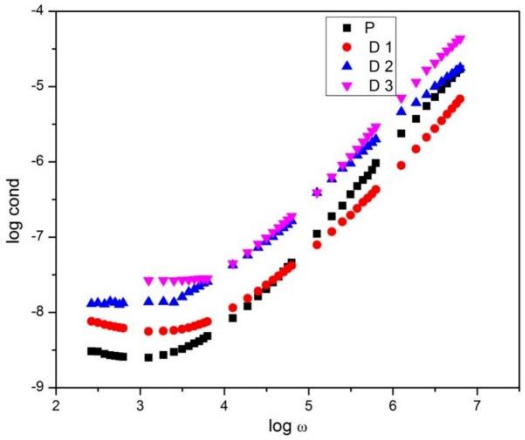

Fig. 8. The conductance spectra of zinc, PVP and silver doped tin oxide nanoparticles.

The conductance spectra of zinc, PVP and silver doped tin oxide nanoparticles are shown in fig. 8. The ionic conductivity is increased for doped samples when compared to pure tin oxide nanoparticles is given in Table 2. The variation of conductivity with respect to the frequency is determined from the correlation of barrier hopping (CBH) model in different doped samples at room temperature[14]. Also, the increasing the conductivity due to the jumping of charge carrier in possible barrier in doped sample and this is occurring due to the defects presented in the sample. The greater number of oxygen vacancies are created due to the increasing concentration of zinc ions replaces the tin ions in the lattice sites[15]. Therefore, the oxygen vacancies are playing the significant role in movement of ions which cause the increasing conductivity for doped samples. Hence, the conductivity is high in high frequency region for doped samples but it is differed for as prepared tin oxide nanoparticles. Therefore, the decrease in dipole moment is observed for pure tin oxide nanoparticles due to the less quantity of oxygen vacancy when compared to doped samples. Therefore, the hopping mechanism is hindered for as prepared tin oxide nanoparticles.

Table 2. The ionic conductivity of pure, Ag, PVP and Zn doped tin oxide nanoparticles

Samples	Ionic conductivity
Pure SnO_2	3.39×10^{-7}
Doped 1	1.54×10^{-7}
Doped 2	2.53×10^{-6}
Doped 3	1.73×10^{-6}

NYQUIST PLOT:

The electrical characterization was studied for as prepared and Ag, PVP and Zn doped tin oxide nanoparticles by AC impedance spectroscopy. The Nyquist plot (cole-cole plot) is used to evaluate the real and complex impedance of pure and Ag, PVP and Zn doped nanoparticles is shown in fig. 9.

Complex impedance : $Z^*(\omega)=(Z'-jZ'')$

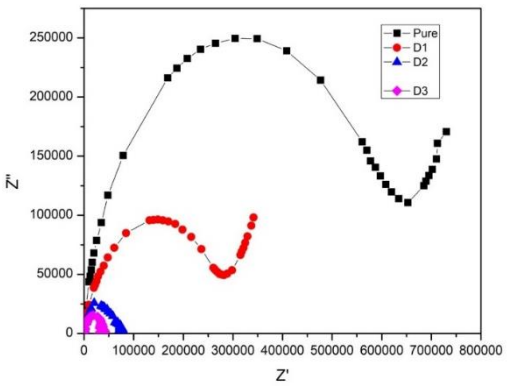

Fig. 9. Cole –Cole plot for prepared samples of pure and Zn, PVP, Silver doped SnO_2 nanoparticles

Fig. 10. represent that the complex impedance plots of as prepared and Zn, PVP and silver doped SnO_2 nanoparticles. The compound plane of Zn, PVP, Silver doped SnO_2 nanoparticles signified by semicircles confirmed the grain effect, grain boundary effect and grain electrode effect. It confirms that impedance spectrum for different doping concentration of Zn in SnO_2 nanoparticles. The certain semicircular array was obtained for every single sample and also noticed that slope of lines decreases with respect to doping concentration and it bends towards the Z' axis.

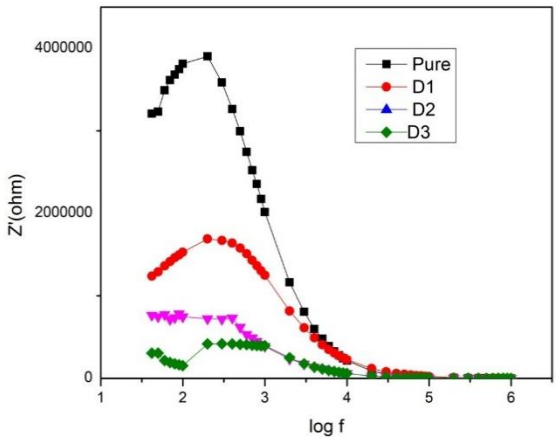

Fig. 10. The variation in real part of impedance (Z')

The variation in real part of impedance (Z') as a function of frequency is shown in fig. 10. It has been observed that Z′ decreases with the increase in frequency for all the compositions. This is due to the increase in conductivity with frequency resulting from hopping phenomenon. It can also be seen from Fig. 9. that Z ′ has strong frequency dependency in the lower frequency region and shows frequency independent behavior in the higher frequency region. Due to the effectiveness of grain boundaries in this region, it attributed to the fact that low frequency region resembles to high conductivity. Moreover, Z ′ decreases with the increasing doping concentration.

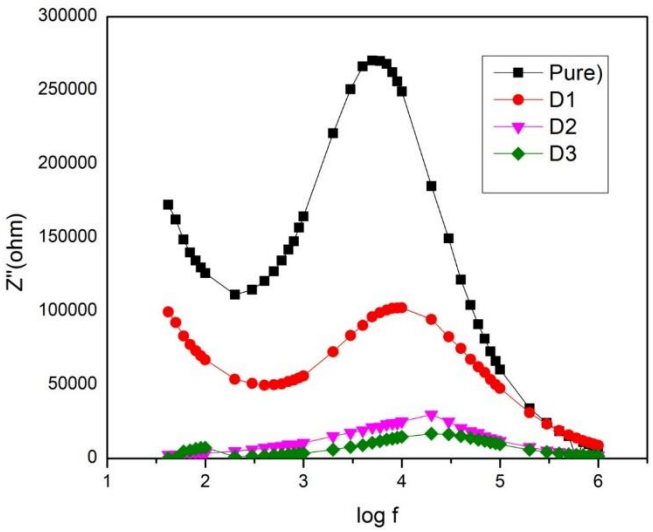

Fig .11 The variation in imaginary part of impedance(Z")

Figure 11 shows the variation of imaginary part of impedance (Z ″) as a function of frequency for pure and Zn, PVP, silver doped nanoparticles. The similar behavior is observed for Z ′ also. Hence, the imaginary part of impedance (Z″) decreases with the increasing concentrations of Zn ions in tin oxide nanoparticles. The PVP may be the reason to decrease the Z' for pure and doped samples. The semicircles in the lower frequency region shows the effect of grain boundaries which enhance the conductivity of nanoparticles in doped samples, PVP and Ag also play the main role to vary the conductivity. The electrical characteristic of a material is studied by the appearance of semicircular arcs in Nyquist plots.

Electric Modulus Spectra Analysis:

The electrode effect can be suppressed by M* formalism. then, electric modulus M' and M" can expressed by the given reaction

$$M^*=1/\varepsilon^*$$

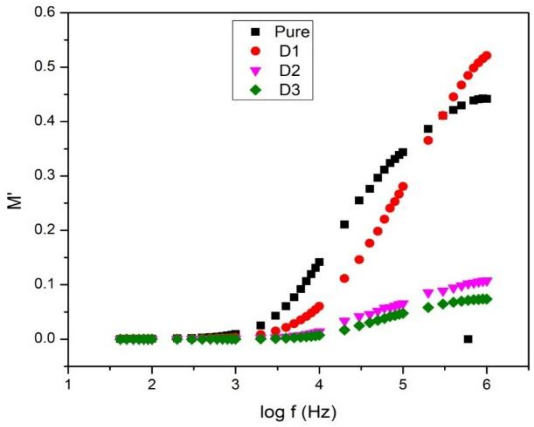

Fig. 12. Variation of M' with frequency for the Zinc, PVP and silver doped tin oxide nanoparticles.

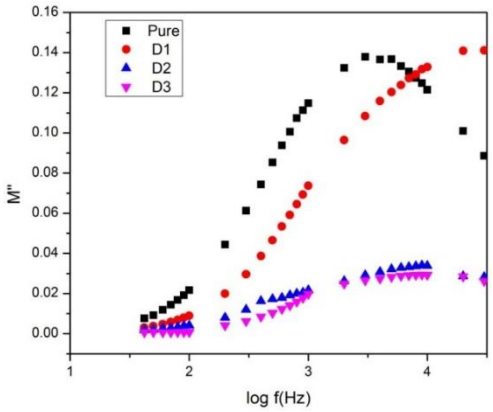

Fig. 13. Variation of M" with frequency for the Zinc, PVP and silver doped tin oxide nanoparticles

Fig. 12 and 13 shows the frequency dependance of the real and imaginary parts of modulus spectra. At higher frequencies the modulus spectrum of Zinc, PVP, and silver doped tin oxide nanoparticles peak was detected. At low frequencies the values of M' and M" approaches zero which indicates that electron polarization is negligible.

IV. Conclusion

Pure and Zn, PVP and Ag doped tin oxide nanoparticles were successfully synthesized by microwave assisted chemical co-precipitation method. The Ag and Zn ions replaced the tin ions in tin oxide lattice sites. Therefore, no zinc and silver peaks are separately detected in XRD pattern. The X-ray diffraction pattern revealed the tetragonal rutile structure of tin oxide for pure and doped nanoparticles. The band gap is increased with increasing concentration of zinc doped tin oxide nanoparticles. The Surface Plasmon resonance peak is observed in UV-Visible absorption spectroscopy due to silver doped tin oxide nanoparticles which enhanced the conductivity of nanoparticles.

References

[1]. Aparna G, Anubhav S, Santanu C, Titash M, Influence of Nanofillers on Adhesion Properties of Polymeric Composites. Acs omega 2022;7:3844−3859.

[2]. Dorel F, Polyblend Nanocomposites, Journal of Macromolecular Science, Part A: Pure and Applied Chemistry,2022 ;52:8, 648-658.

[3]. Mei G, Li Z, Yi Z, Qin Z, Yanying W, Li W, Yubao L, Investigation on the Interpenetrating Polymer Networks (IPNs) of Polyvinyl Alcohol and Poly (N-vinyl pyrrolidone) Hydrogel and Its In Vitro Bioassessment. Journal of Applied Polymer Science, 2012; 125, 2799–2806.

[4]. Rabia J, Muhammad Z, Sania N, Samson O. A, Noorul A, Qiang A, Role of capping agents in the application of nanoparticles in biomedicine and environmental remediation: recent trends and future prospects, 2020;18:172.

[5]. Kallum M. K, Stefanos M, Lakshminarayana P, Sara E, Polyvinylpyrrolidone (PVP) in nanoparticle synthesis Dalton Transactions. 2015; 1-22.
[6]. M. T. Ramesan, Meghana V, Jayakrishnan P, Pradeepan P, Silver-Doped Zinc Oxide as a Nanofiller for Development of Poly(vinyl alcohol)/Poly(vinyl pyrrolidone) Blend Nanocomposites, Advances in Polymer Technology, 2016.
[7]. T. Siva V, S. Karthikeyeni, S. Vasanth, Arul G, G. Bupesh, R. Ramesh, M. Manimegalai, P. Subramanian, Journal of Nanoscience 2013.
[8]. Nadia M K, Farzaneh S, Green Facile Synthesis of Silver-Doped Zinc Oxide Nanoparticles and Evaluation of Their Effect on Drug Release, Materials 2022; 15, 5536.
[9]. Hassan A S, Oluwaseun A, Maroof A K, Paramasivam S, Ismaila T B, Sonachalam A, Effect of Low-Doping Concentration on Silver-Doped SnO_2 and its Photocatalytic Applications, Biointerface Reserch in Applied Chemistry, 2023; 13, 165.
[10]. Payam M, Mohammad H, Sono-Coprecipitation Synthesis and Physicochemical Characterization of CdO - ZnO Nano photo catalyst for Removal of Acid Orange 7 from Wastewater, Ultrasonics Sonochemistry, 2017.
[11]. Krzysztof C. K, Charles M. L, Nanocomposites Prepared by Sol-Gel Methods: Synthesis And Characterization, 2000.
[12]. Nguyen T. K. T, N. Maclean, S. Mahiddine, Mechanisms of Nucleation and Growth of Nanoparticles in Solution, Chem. Rev. 2014, 114, 7610−7630.
[13]. J. Mayandi, M. Marikkannan, V. Ragavendran, P. Jayabal, Hydrothermally Synthesized Sb and Zn Doped SnO_2 Nanoparticles, Journal of NanoScience and NanoTechnology, 2014, 2279 – 0381
[14]. Rajkumar J, Joydeep D, Sayantan S, Arka D, Baishakhi P, Animesh B, Partha P R, Exploration of temperature dependent dielectric relaxation and correlated barrier hopping (CBH) conduction mechanism of hydrothermally synthesized CuO nanoflakes, Mater. Res. Express 6, 2019; 1050d1.
[15]. A. Amutha et al., Facile Synthesis and Characterization of Microstructure and Optical Properties of Pure and Zn Doped SnO2 Nanorods, Journal of Cluster Science, 2021.